Received: 11 November 2021 | Accepted: 23 December 2021

DOI: 10.1111/1759-7714.14310

ORIGINAL ARTICLE

WILEY

Circ_0001955 plays a carcinogenic role in breast cancer via positively regulating GLUT1 via decoying miR-1299

Hong Cheng[1] | **Sijie Kuang**[2] | **Lingzhen Tan**[2] | **Shengrong Sun**[1]

[1]Department of Breast and Thyroid Surgery, Renmin Hospital of Wuhan University, Wuhan City, Hubei, China

[2]Department of Breast Surgery, The Central Hospital of Enshi Tujia and Miao Autonomous Prefecture, Enshi City, Hubei Province, China

Correspondence
Shengrong Sun, Department of Breast and Thyroid Surgery, Renmin Hospital of Wuhan University, No. 238 Ziyang Road, Wuhan, 430060, Hubei, China.
Email: sun136971@126.com

Abstract

Background: Breast cancer is widespread in females. The role of circular RNA (circRNA) in breast cancer has aroused much attention. However, the function of several circRNAs remain unclear. The aim of our study was to determine the role of circ_0001955 in breast cancer.

Methods: Quantitative real-time PCR (qPCR) and western blot was employed for expression analysis of circ_0001955, miR-1299 and glucose transporter 1 (GLUT1). Cell functions including proliferation, apoptosis, migration, invasion and angiogenesis, were assessed using EdU, flow cytometry, transwell and tube formation assays. Glycolysis metabolism was assessed according to glucose consumption, lactate production and ATP content. Dual-luciferase reporter assay and RIP assay were utilized to validate the binding between miR-1299 and circ_0001955 or GLUT1. The effects of circ_0001955 in vivo were observed by animal study.

Results: Upregulation of circ_0001955 was detected in breast cancer. Knockdown of circ_0001955 inhibited breast cancer cell proliferation, migration, invasion, angiogenesis and glycolysis. MiR-1299 was a target of circ_0001955, and its repression reversed the effects of circ_0001955 knockdown. Moreover, circ_0001955 targeted miR-1299 to positively regulate GLUT1 expression. GLUT1 overexpression reversed the effects of miR-1299 enrichment. GLUT1 knockdown was verified to block tumor growth in vivo.

Conclusions: Circ_0001955 was found to promote breast cancer malignant development via targeting of the miR-1299/GLUT1 pathway, which contributes to our understanding of the pathogenesis of breast cancer.

KEYWORDS
breast cancer, circ_0001955, GLUT1, miR-1299

INTRODUCTION

Female breast cancer is the most common cancer in women, and a total of 2.3 million new cases were diagnosed in 2020.[1] The incidence rate of breast cancer is rapidly increasing, leading to a low survival rate.[1] The pathogenesis of breast cancer is complex, with poor therapeutic outcomes due to disease heterogeneity, therapeutic target variety, therapeutic resistance, metastasis and recurrence.[2] The understanding of breast cancer biology reports that molecular anomaly, such as the deregulation of oncogenes, tumor suppressor genes and oncogenic signaling pathways, is closely related to the development of cancer.[3–5] Therefore, the study of dysregulated molecules in breast cancer may be conducive to the understanding of molecular anomaly in cancer development.

Circular RNAs (circRNAs) are a class of non-coding RNA molecules characterized by closed-loop structures. These special RNAs widely exist in mammals and take part in various cancer-related cellular processes, such as proliferation, angiogenesis, metastasis, drug resistance and energy metabolism.[6,7] Relative to linear transcripts, circRNAs harbor no free 5′ and 3′ terminals in structure and thus have higher stability,[8] which make circRNAs more advantageous as biomarkers. CircRNAs that function as oncogenes or

tumor suppressor genes have been widely revealed in breast cancer. For example, circKIF4A has been found to be upregulated in breast cancer, and its absence repressed cancer cell proliferation and migration.[9] In contrast, circ_0025202 has been reported to be downregulated in breast cancer, and circ_0025202 overexpression blocked cancer cell proliferation, migration and drug-resistance.[10] Various circRNAs exert different functional pattern in cancer development, and the study of these oncogenic drivers or tumor suppressors provides a basis for targeted therapies. CircRNA sequencing profile identifies a large number of circRNAs that are differently expressed in breast cancer. However, the function of numerous circRNAs in this disorder remain unknown. Here, we analyzed circRNA microarray from the public GEO database and identified the upregulation of circ_0001955 in breast tumor tissues in the GSE101123 dataset, which implies the involvement of circ_0001955 in breast cancer. However, the detailed functions of circ_0001955 have not yet been fully explored.

CircRNAs attract a great deal of research attention because they may contribute to gene regulation through a variety of roles, including functioning as an miRNA sponge, interacting with RNA-binding proteins, regulation of transcription and splicing, and protein translation.[11] Importantly, circRNAs function as an miRNA sponge to decoy miRNA and correspondingly regulate the expression of downstream genes.[12] For instance, circ_0025202 acted as miR-182-5p sponge to further modulate the expression and activity of FOXO3a.[10] With the application of circRNA-specific bioinformatics databases,[13,14] miRNAs potentially targeted by certain circRNA are easily predicted. Thereupon, miR-1299 was predicted to be a target of circ_0001955, and miR-1299 bound to glucose transporter 1 (GLUT1) 3′UTR to suppress GLUT1 expression. However, the relationship between circ_0001955, miR-1299 and GLUT1 has not yet been clarified. It is therefore of significance to investigate whether miR-1299 and GLUT1 are involved in circ_0001955 regulatory networks.

The present study investigated the functions of circ_0001955 in breast cancer cell malignant behaviors and in animal models. In addition, we addressed the interaction between miR-1299 and circ_0001955 or GLUT1 in cancer progression, so as to provide a new mechanism regarding the function of circ_0001955 in breast cancer.

METHODS

Clinical tissues

All tissues, including cancer tissues ($n = 51$) and adjacent normal tissues ($n = 51$), were excised from patients with breast cancer who underwent surgery at The Central Hospital of Enshi Tujia and Miao Autonomous Prefecture. None of the patients had previously undergone chemotherapy or radiotherapy. All patients had signed their written informed consent. Tissues excised from bodies were treated with liquid nitrogen and stored at −80°C freezer. All procedures were approved by the Ethics Committee of The Central Hospital of Enshi Tujia and Miao Autonomous Prefecture.

TABLE 1 Primer sequences used in this study

Name	Primers for PCR (5′–3′)
circ_0001955	
Forward	ACTCGAGAAAGCCACACACA
Reverse	CTCCAGCACCATGGCATTAT
CSNK1G1	
Forward	GGAAAGAGAGAAACCACCGC
Reverse	TTGTAACCTGGTCCAGCAGT
GLUT1 (SLC2A1)	
Forward	GAGCAGCTACCCTGGATGTC
Reverse	GGAAGCACATGCCCACAATG
miR-1299	
Forward	GTATGATTCTGGAATTCTGTGT
Reverse	CTCAACTGGTGTCGTGGAG
β-Actin	
Forward	CTTCGCGGGCGACGAT
Reverse	CCACATAGGAATCCTTCTGACC
U6	
Forward	CTCGCTTCGGCAGCACA
Reverse	AACGCTTCACGAATTTGCGT

Cell lines and cell culture

MDA-MB-453, SKBR3 and MCF-10A cells were all obtained from TongPai Biotechnology (Shanghai, China) and cultured in Leibovitz-15 (with 10% FBS), McCoy's 5A (with 10% FBS) and DMEM (with 10% FBS), respectively. A temperature incubator (37°C) supplemented with 5% CO_2 was used to culture the cells.

Quantitative real-time PCR (qPCR)

Total RNA was isolated from samples with the use of a Trizol reagent (Sigma-Aldrich). Afterwards, reverse transcription was implemented according to the instructions from a PrimeScript RT reagent Kit (Takara) or miRcute Plus miRNA First-Strand cDNA Kit (TianGen), followed by qPCR amplification using a SYBR Premix Ex Taq (Takara). Herein, we adopted β-actin or U6 to normalize the data. Relative expression was processed by $2^{-\triangle\triangle Ct}$ method. Primer sequences are listed in Table 1.

RNase R treatment

Total RNA was isolated, exposed to RNase R (BioVision) for 30 min at 37°C and the treated RNA was then subjected to qPCR.

Subcellular location assay

To determine the distribution of circ_0001955 in cytoplasm or in nucleus, cytoplasmic RNA and nuclear RNA were separately isolated from MDA-MB-453 and SKBR3 cells using the PARIS kit (Thermo Fisher). RNA from different fractions was then subjected to qPCR.

Cell transfection

Small interference RNA (siRNA) targeting circ_0001955, including si-circ_0001955$^{\#1}$ and circ_0001955$^{\#2}$, and matched scramble control (si-NC) were provided by Ribobio. The mimic and inhibitor of miR-1299 (miR-1299 and in-miR-1299) and matched negative controls (miR-con and in-miR-con) were purchased from Ribobio. GLUT1 sequence was cloned into pcDNA vector for GLUT1 overexpression (GLUT1) by Tsingke. Cell transfection was implemented with the use of lipofectamine 3000 reagent (Invitrogen).

EdU assay

As previously mentioned,[15] EdU assay was performed using the EdU incorporation proliferation assay kit (Beyotime). Cell nucleus was stained using DAPI (Beyotime). All staining was observed under a fluorescence microscope (Nikon).

Western blot assay

Total protein separated by 10% SDS-PAGE was transferred onto PVDF membranes (Beyotime). Membranes were subsequently exposed to 5% nonfat milk for protein blocking. The primary antibodies, such as anti-PCNA (ab92552; Abcam), anti-GLUT1 (ab115730) and anti-β-actin (ab8227), were used to culture membranes overnight at 4°C. HRP-conjugated secondary antibody (ab205718) was next used to culture membranes for 2 h at room temperature. Finally, an ECL kit (Beyotime) was utilized to visualize protein signals.

Wound healing assay

Cells were seeded into 24-well plates (5×10^4 cell/well) and then maintained at 37°C overnight. At 90% of cell confluence, cell surface was scratched with a sterile pipette tip to mimic a wound. Photographs of wound distance were immediately recorded using light microscopy. After culturing cells for 24 h, wound distance was again recorded by light microscopy.

Transwell assay

Transwell chambers coated with matrigel were used for invasion analysis. In brief, a total of 5×10^4 cells were collected into serum-depleted culture medium and then supplemented into the top of chambers. Meantime, the lower chambers were added with matched culture medium containing 20% FBS. Cells in chambers were induced to invade for 24 h. Subsequently, cells across the membrane to the lower surface of chambers were fixed with methanol and stained with crystal violet. Five random fields were used to count the number of cells under a microscope (Nikon; 100× amplification).

Flow cytometry assay

At 48 h after transfection, cells were collected and administered with an Annexin V-FITC Apoptosis Detection Kit (Beyotime). In brief, cells were resuspended in Annexin V-FITC binding buffer and then stained using Annexin V-FITC and propidium iodide (PI). The apoptotic cells were identified using a flow cytometer (Beckman Coulter).

Tube formation assay

The conditioned culture medium of MDA-MB-453 and SKBR3 cells with various transfections was collected. Human umbilical vein endothelial cells (HUVECs) cultured in the conditioned culture medium were then plated into 96-well plates coated with matrigel (2×10^4 cells/well). After incubation for 6 h, the capillary structure was observed under a microscope (Nikon).

Glycolysis assessment

Glucose consumption, lactate production and ATP content were investigated using glucose assay, lactate assay and ATP assay kits, all purchased from Sigma-Aldrich. According to the different instructions, these indexes were determined to assess oxidative stress.

Dual-luciferase reporter assay

The potential binding site between circ_0001955 and miR-1299 was predicted by circular RNA Interactome (https://circinteractome.nia.nih.gov/) and circAtlas (http://circatlas.biols.ac.cn/). Next, the wild-type (WT) and mutant-type (MUT) sequence fragments of circ_0001955 were generated and constructed into pmirGlO vector. Likewise, the potential binding site between miR-1299 and GLUT1 3′UTR was predicted by microT-CDS (http://diana.imis.athena-innovation.gr/DianaTools/index.php?r=microT_CDS/index), and the WT and MUT sequence fragments of GLUT1 3′UTR were also generated and cloned into pmirGLO vector. The fusion reporter vectors were respectively transfected with miR-1299 or miR-con into MDA-MB-453 and SKBR3 cells, and cells were cultured for 48 h. Afterwards, luciferase activity was examined using a dual-luciferase reporter assay system (Promega).

RIP assay

Using a Magna RIP RNA-binding protein immunoprecipitation kit (Emd Millipore), cell lysates were prepared. Magnetic beads were preincubated with anti-Ago2 or anti-IgG. Cell lysates were incubated with bead-antibody complexes. RNA compounds precipitated into beads were eluted and isolated using trizol reagent. The expression of circ_0001955, miR-1299 and GLUT1 was checked by qPCR.

Animal model

Xenograft model was established in nude mice (balb/c, female, 6-week-old) purchased from Vital River Laboratory Animal (Beijing, China). In brief, short-hairpin RNA targeting circ_0001955 (sh-circ_0001955) and matched control (sh-con) were synthesized and inserted into lentiviral vector by Geneseed. Nude mice were housed and randomly divided into three groups ($n = 6$ per group) and subcutaneously injected with SKBR3 cells infected with lentiviral-packaged sh-circ_0001955 or sh-con. Nude mice in the mock group were only subcutaneously injected with SKBR3 cells. One week later, tumor volume was measured once a week (length × width^2 × 1/2). Then, 4 weeks later, the nude mice were killed to remove tumor tissues for further analysis. All animal study procedures were approved by the Animal Care and Use Committee of The Central Hospital of Enshi Tujia and Miao Autonomous Prefecture.

Statistical analysis

The experimental data were obtained from three independent experiments. Data processing and statistical analysis were implemented using GraphPad Prism 5.0 (GraphPad).

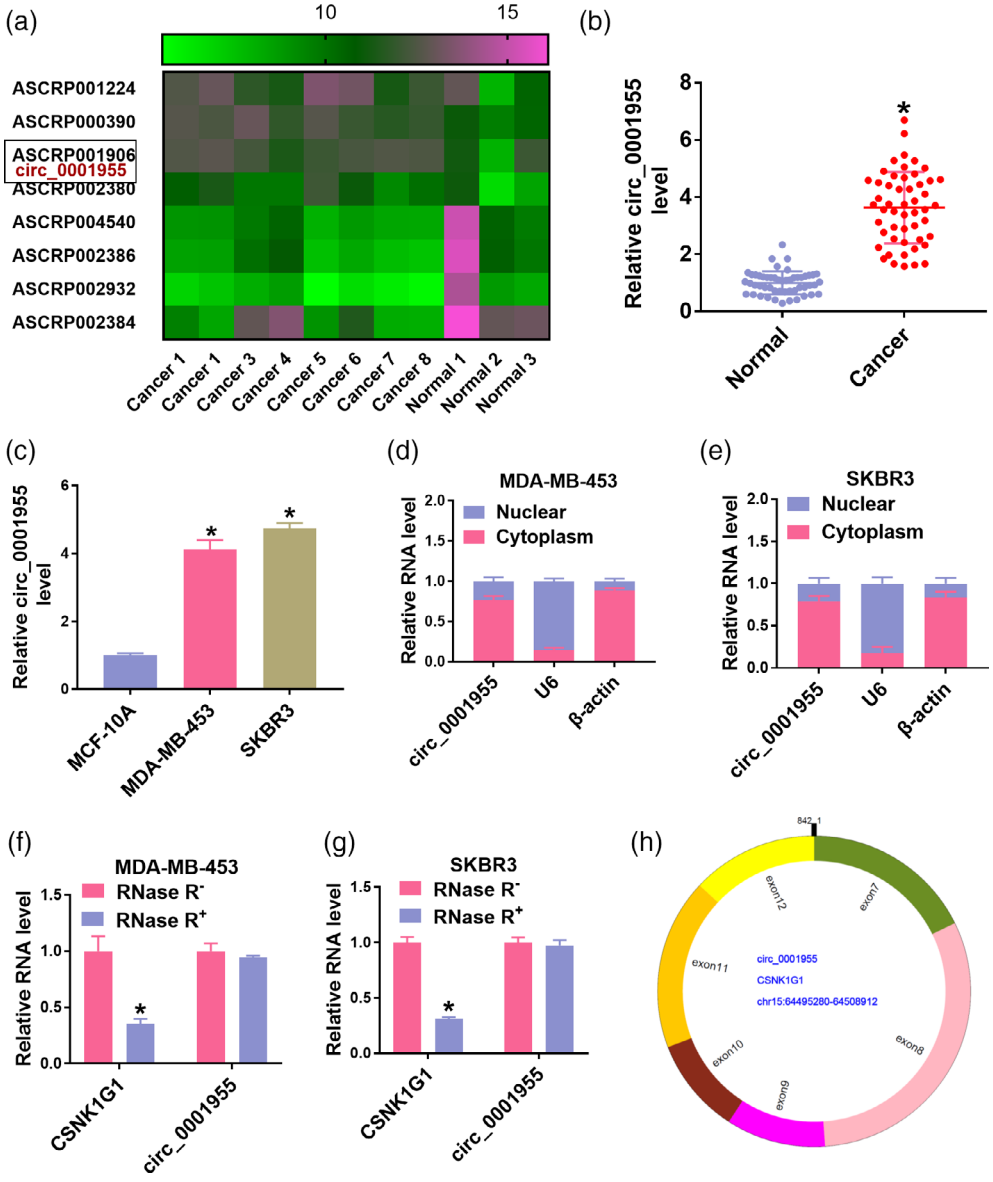

FIGURE 1 Circ_0001955 was highly expressed in breast cancer. (a) A GEO dataset showed that circ_0001955 was one of the upregulated circRNAs in breast cancer. (b) Circ_0001955 expression in cancer tissues and normal tissues was detected by qPCR. (c) Circ_0001955 expression in MCF-10A, MDA-MB-453 and SKBR3 cells was detected by qPCR. (d–e) Subcellular location of circ_0001955. (f, g) the existence of circ_0001955 was verified using RNase R. (h) The production of circ_0001955 from CSNK1G1 gene. *$p < 0.05$

For correlation analysis, Pearson's analysis was utilized. For difference comparison, Student's *t*-test or analysis of variance was utilized as appropriate. Data are expressed as the mean ± standard deviation, and *p*-values <0.05 were considered statistically significant.

RESULTS

Circ_0001955 expression upregulated in breast cancer tissues and cells

A circRNA expression profile presented that circ_0001955 was one of the upregulated circRNAs in breast cancer tissues ($n = 8$) relative to normal tissues ($n = 3$) (Figure 1a). We then validated the expression of circ_0001955 in clinical samples and cell lines. As shown in Figure 1b, c, circ_0001955 expression was strikingly higher in cancer tissues and cancer cell lines (MDA-MB-453 and SKBR3) relative to normal tissues and non-cancer cells (MCF-10A), respectively. Circ_0001955 was principally distributed in the cytoplasm but not in the nucleus (Figure 1d, e). The resistance of circ_0001955 to RNase R confirmed the existence of circ_0001955 (Figure 1f, g). The production of circ_0001955 from CSNK1G1 was displayed in Figure 1h, showing that circ_0001955 was derived from the exon7-exon12 regions of CSNK1G1 gene.

Circ_0001955 deficiency suppressed breast cancer cell malignant phenotypes

Two siRNA oligos targeting circ_0001955 were synthesized to mediate circ_0001955 knockdown, and circ_0001955 expression was notably decreased in MDA-MB-453 and SKBR3 cells with si-circ_0001955$^{\#1}$ or si-circ_0001955$^{\#2}$ transfection (Figure 2a). The transfection of si-circ_0001955$^{\#2}$ resulted in a lower level of circ_0001955, and thus cells transfected with si-circ_0001955$^{\#2}$ were used in the following assays. By EdU assay, circ_0001955 knockdown markedly reduced the number of EdU-positive cells (Figure 2b, c), hinting that circ_0001955 knockdown blocked cell proliferation, which was verified by the decreased level of PCNA in si-circ_0001955$^{\#2}$-transfected cells (Figure 2d, e). Wound healing and transwell assays showed that cell migration and cell invasion were

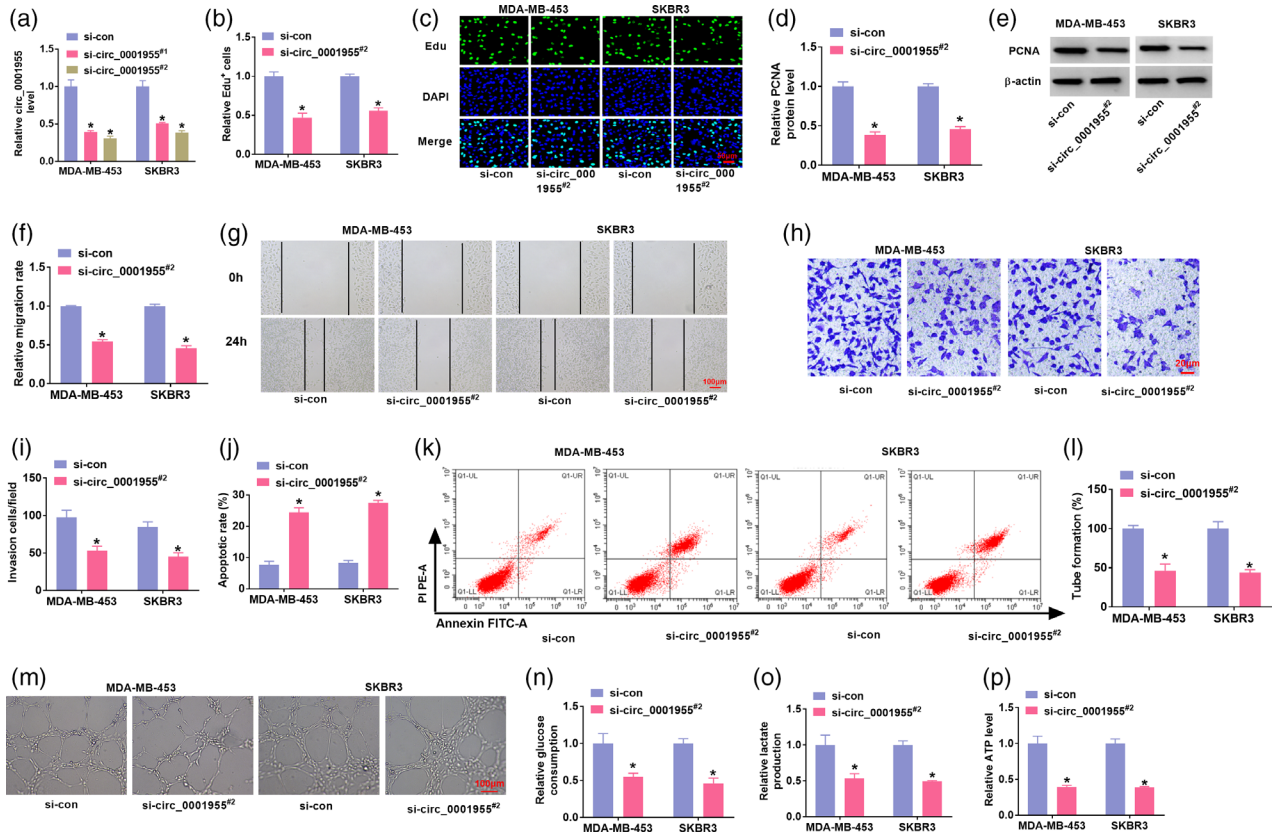

FIGURE 2 Circ_0001955 knockdown attenuated breast cancer cell proliferation, migration, invasion, angiogenesis and glycolysis. (a) The efficiency of si-circ_0001955$^{\#1}$ and si-circ_0001955$^{\#2}$ was checked by qPCR. (b, c) The role of circ_0001955 on cell proliferation was assessed by EdU assay. (d, e) PCNA expression was detected by western blot to assess cell proliferation. (f, –i) The role of circ_0001955 on cell migration and cell invasion was assessed by wound healing and transwell assays. (j, k) The role of circ_0001955 on cell apoptosis was identified by flow cytometry assay. (l, m) The role of circ_0001955 on angiogenesis was evaluated by tube formation assay. (n–p) The role of circ_0001955 on glycolysis metabolism was assessed by monitoring glucose consumption, lactate production and ATP level. *$p < 0.05$

considerably repressed by si-circ_0001955$^{\#2}$ transfection (Figure 2f–i). Knockdown of circ_0001955 strongly promoted the apoptotic rate of MDA-MB-453 and SKBR3 cells by flow cytometry assay (Figure 2j, k). In addition, circ_0001955 knockdown inhibited angiogenesis of MDA-MB-453 and SKBR3 cells via tube formation assay (Figure 2l, m). Moreover, the levels of glucose consumption, lactate production and ATP were remarkably suppressed by circ_0001955 knockdown in MDA-MB-453 and SKBR3 cells (Figure 2n–p). All data supported that circ_0001955 knockdown blocked breast cancer cell malignant development.

MiR-1299, targeted by circ_0001955, downregulated in breast cancer

A total of 5 miRNAs targeted by circ_0001955 were commonly predicted by the circular RNA interactoma and circAtlas 2.0 public databases (Figure S1). We then performed a pulldown assay and used circ_0001955 probe to enrich the potential miRNAs. As a result, miR-1299 showed the highest abundance compared to other miRNAs (Figure S1B, C), and miR-1299 was thus chosen in our study. Circ_0001955 contained a special binding site with miR-1299 (Figure 3a). The WT and MUT constructs of circ_0001955 were generated for dual-luciferase reporter assay, showing that luciferase activity was notably lessened in cells by miR-1299 and circ_0001955-WT cotransfection (Figure 3b, c). In addition, both circ_0001955 and miR-1299 could be abundantly enriched by anti-Ago2 antibody in the RIP assay, suggesting that the binding between circ_0001955 and miR-1299 might be mediated by Ago2 (Figure 3d, e). MiR-1299 expression was strikingly lower in cancer tissues relative to normal tissues (Figure 3f), and miR-1299 expression showed negative correlation with circ_0001955 expression in cancer tissues (Figure 3g). MiR-1299 expression was also reduced in MDA-MB-453 and SKBR3 cells relative to MCF-10A cells (Figure 3h), and its expression was reinforced in MDA-MB-453 and SKBR3 cells after circ_0001955 knockdown (Figure 3i).

MiR-1299 inhibition reversed the functional role of circ_0001955 deficiency

Transfection of in-miR-1299 significantly weakened miR-1299 expression in MDA-MB-453 and SKBR3 cells

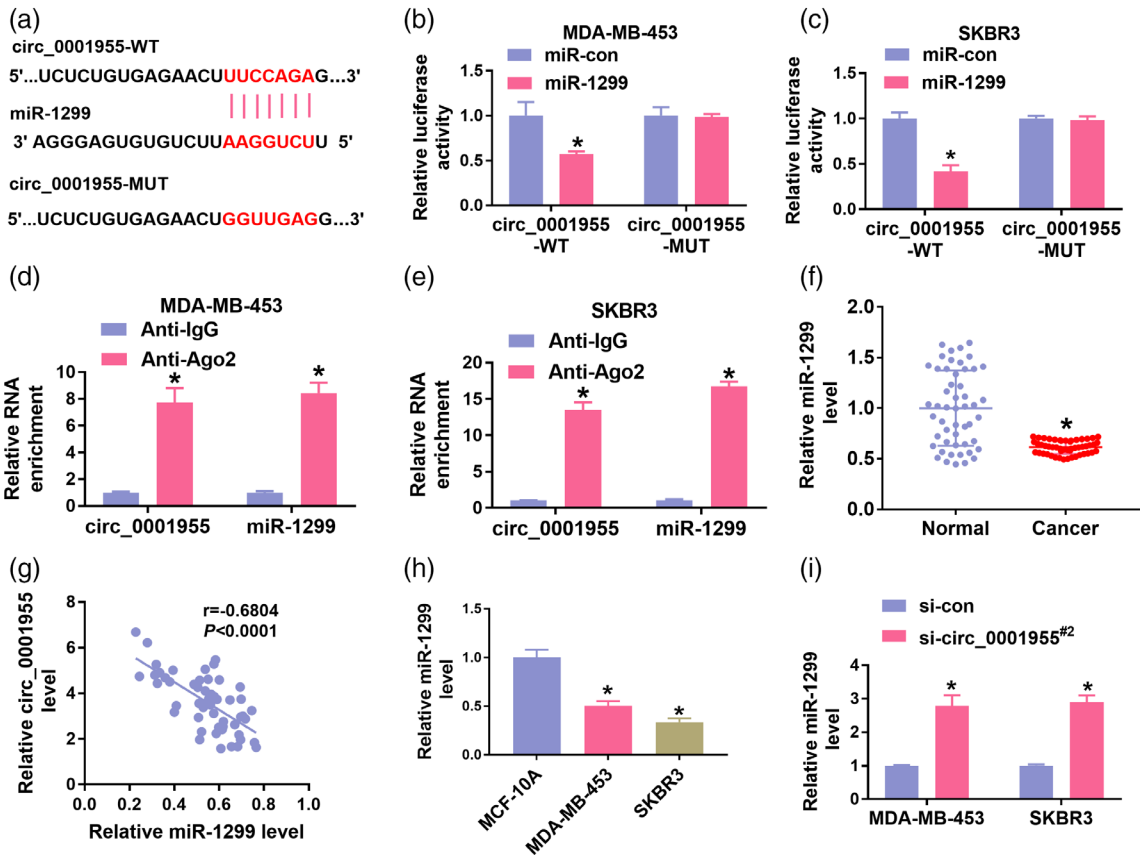

FIGURE 3 Circ_0001955 bound to miR-1299. (a) The predicted binding site between circ_0001955 and miR-1299. (b, c) Their binding was validated by dual-luciferase reporter assay. (d, e) The binding between circ_0001955 and miR-1299 was validated by RIP assay. (f) MiR-1299 expression in breast cancer tissues and normal tissues was detected by qPCR. (g) The correlation between miR-1299 expression and circ_0001955 expression in cancer tissues. (h) MiR-1299 expression in MCF-10A, MDA-MB-453 and SKBR3 cells was detected by qPCR. (i) MiR-1299 expression in MDA-MB-453 and SKBR3 cells after circ_0001955 knockdown was detected by qPCR. *$p < 0.05$

(Figure 4a, b). Then, miR-1299 expression was notably enhanced in cells transfected with si-circ_0001955$^{\#2}$, while its expression was repressed in cells transfected with si-circ_0001955$^{\#2}$ + in-miR-1299 (Figure 4c, d). In function, the inhibitory effects of circ_0001955 knockdown on cell proliferation, migration, invasion and angiogenesis were all reversed by the inhibition of miR-1299 (Figure 4e–l, o, p). In addition, si-circ_0001955$^{\#2}$-induced cell apoptosis was largely alleviated by si-circ_0001955$^{\#2}$ + in-miR-1299 in MDA-MB-453 and SKBR3 cells (Figure 4m, n). Inhibition of glucose consumption, lactate production and ATP content caused by circ_0001955 knockdown in MDA-MB-453 and SKBR3 cells was also largely restored by additional miR-1299 deficiency (Figure 4q–v). The data introduced that circ_0001955 deficiency suppressed breast cancer cell proliferation, migration, invasion, angiogenesis and glycolysis via upregulating miR-1299.

MiR-1299 binding between GLUT1 3′UTR

By the prediction of microT-CDS, miR-1299 contained a special binding site with GLUT1 3′UTR (Figure 5a). The binding between miR-1299 and GLUT1 3′UTR was then verified by dual-luciferase reporter assay and RIP assay, showing the decrease of luciferase activity in MDA-MB-453 and SKBR3 cells transfected with miR-1299 and GLUT1-3′UTR-WT and the enrichment of GLUT1 and miR-1299 in anti-Ago2-governed RIP group (Figure 5b–e). The expression of GLUT1 mRNA was notably elevated in cancer tissues and showed negative correlation with miR-1299 expression (Figure 5f, g). The expression of GLUT1 protein was also markedly increased in cancer tissues and cell lines (Figure 5h, i). Moreover, miR-1299 expression was enriched in MDA-MB-453 and SKBR3 cells transfected with miR-1299 (Figure 5j), and the enrichment of miR-1299 in MDA-MB-453 and SKBR3 cells significantly reduced the

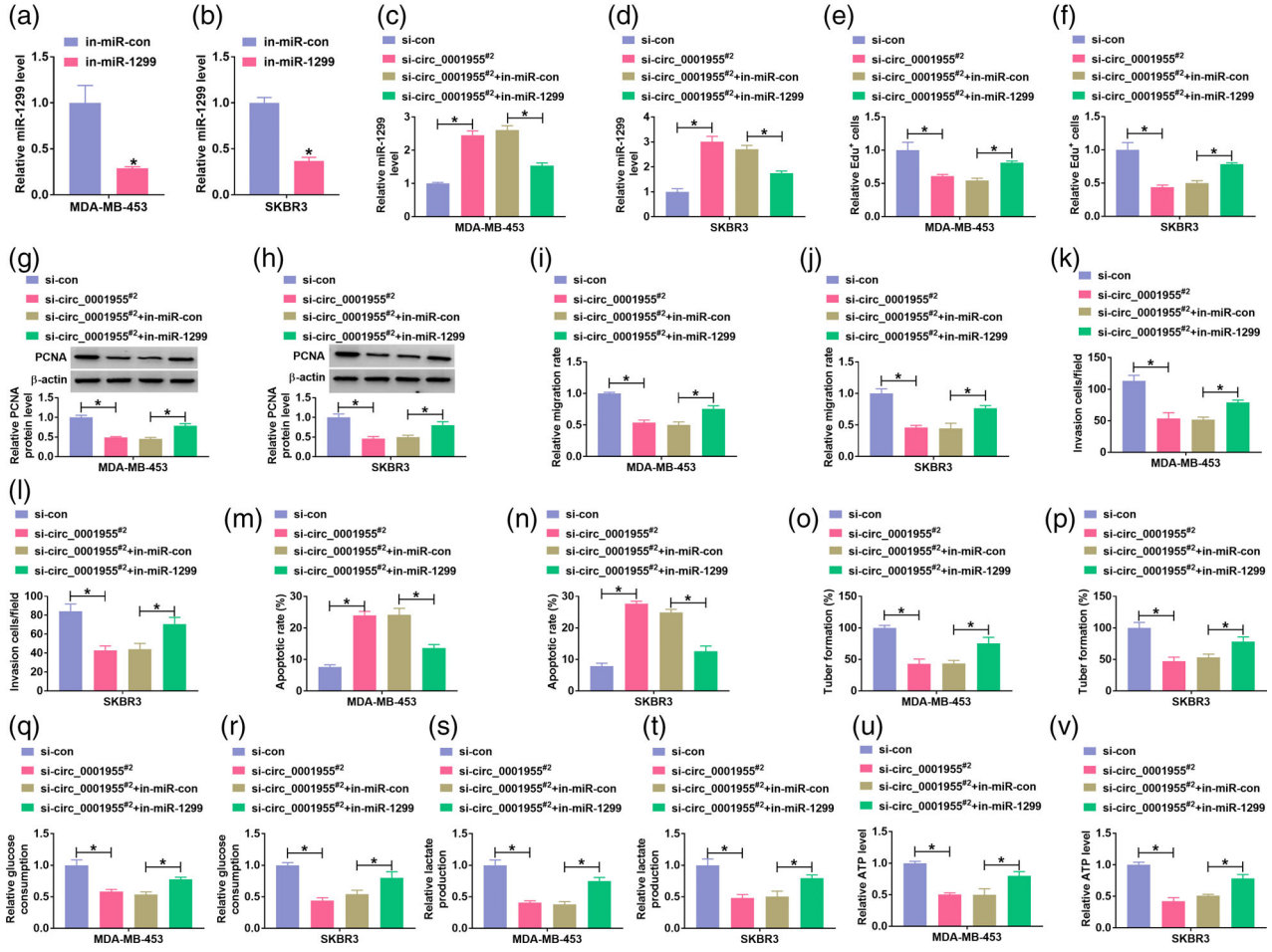

FIGURE 4 MiR-1299 inhibition reversed the effects of circ_0001955 knockdown. (a, b) the efficiency of in-miR-1299 was examined by qPCR. (c, d) in MDA-MB-453 and SKBR3 cells transfected with si-circ_0001955$^{\#2}$ or si-circ_0001955$^{\#2}$ + in-miR-1299, miR-1299 expression was measured by qPCR. (e, f) Cell proliferation in these cells was evaluated by EdU assay. (g, h) PCNA expression detected by western blot was used to assess cell proliferation. (i–l) Cell migration and cell invasion in these cells were evaluated by wound healing assay and transwell assay. (m, n) Cell apoptosis in these cells was evaluated by flow cytometry assay. (o, p) Angiogenesis in these cells was assessed by tube formation assay. (q–v) Glycolysis metabolism in these cells was evaluated by glucose consumption, lactate production and ATP level. *$p < 0.05$

expression of GLUT1 (Figure 5k). The data verified that GLUT1 was a target of miR-1299.

GLUT1 overexpression reversed the functional role of miR-1299 enrichment

The use of GLUT1 overexpression vector considerably enhanced the expression of GLUT1 protein in MDA-MB-453 and SKBR3 cells (Figure 6a, b). Then, GLUT1 expression was notably weakened in MDA-MB-453 and SKBR3 cells transfected with miR-1299, while its expression was restored in cells transfected with miR-1299 + GLUT1 (Figure 6c, d). In function, miR-1299 enrichment-inhibited cell proliferation was recovered by GLUT1 reintroduction (Figure 6e, f), which was verified by the enhanced expression of PCNA in MDA-MB-453 and SKBR3 cells miR-1299 + GLUT1 (Figure 6g, h). Besides, miR-1299 enrichment-blocked cell migration and cell invasion were also promoted by GLUT1 overexpression (Figure 6i, l; Figure S2). In contrast, miR-1299 upregulation-induced cell apoptosis was relieved by the reintroduction of GLUT1 (Figure 6m, n; Figure S2). MiR-1299 enrichment also suppressed tube formation ability of MDA-MB-453 and SKBR3 cells, while

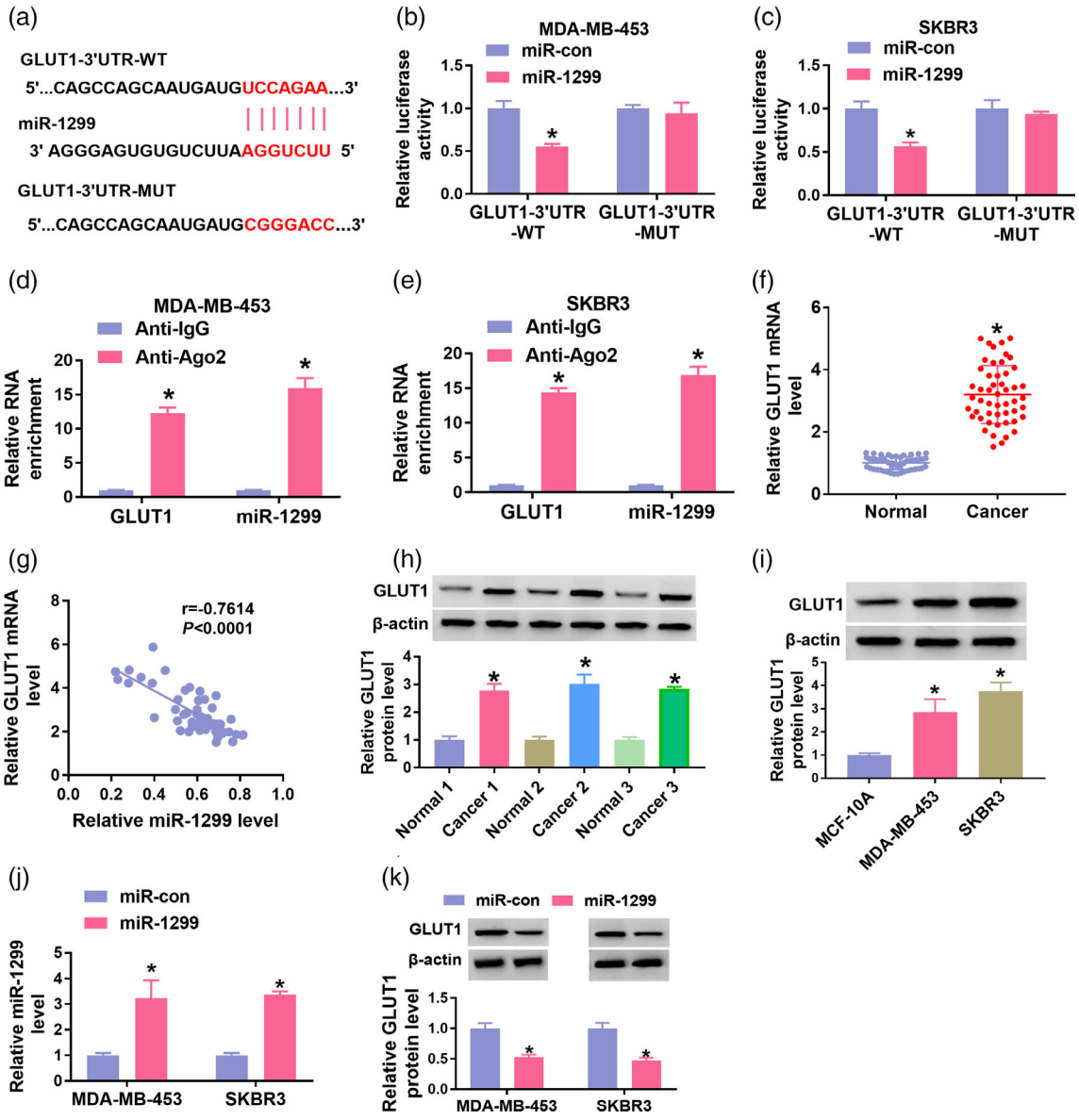

FIGURE 5 MiR-1299 bound to GLUT1 3′UTR. (a) The predicted binding site between miR-1299 and GLUT1 3′UTR. (b, c) The binding site between miR-1299 and GLUT1 was confirmed by dual-luciferase reporter assay. (d, e) The binding between miR-1299 and GLUT1 was confirmed by RIP assay. (f) GLUT1 expression in cancer tissues and normal tissues was detected by qPCR. (g) The correlation between GLUT1 expression and miR-1299 expression. (h) GLUT1 expression in cancer tissues and normal tissues was detected by western blot. (i) GLUT1 expression in MCF-10A, MDA-MB-453 and SKBR3 cells was measured by western blot. (j) The efficiency of miR-1299 mimic was checked by qPCR. (k) GLUT1 expression in MDA-MB-453 and SKBR3 cells after miR-1299 enrichment was measured by western blot. *$p < 0.05$

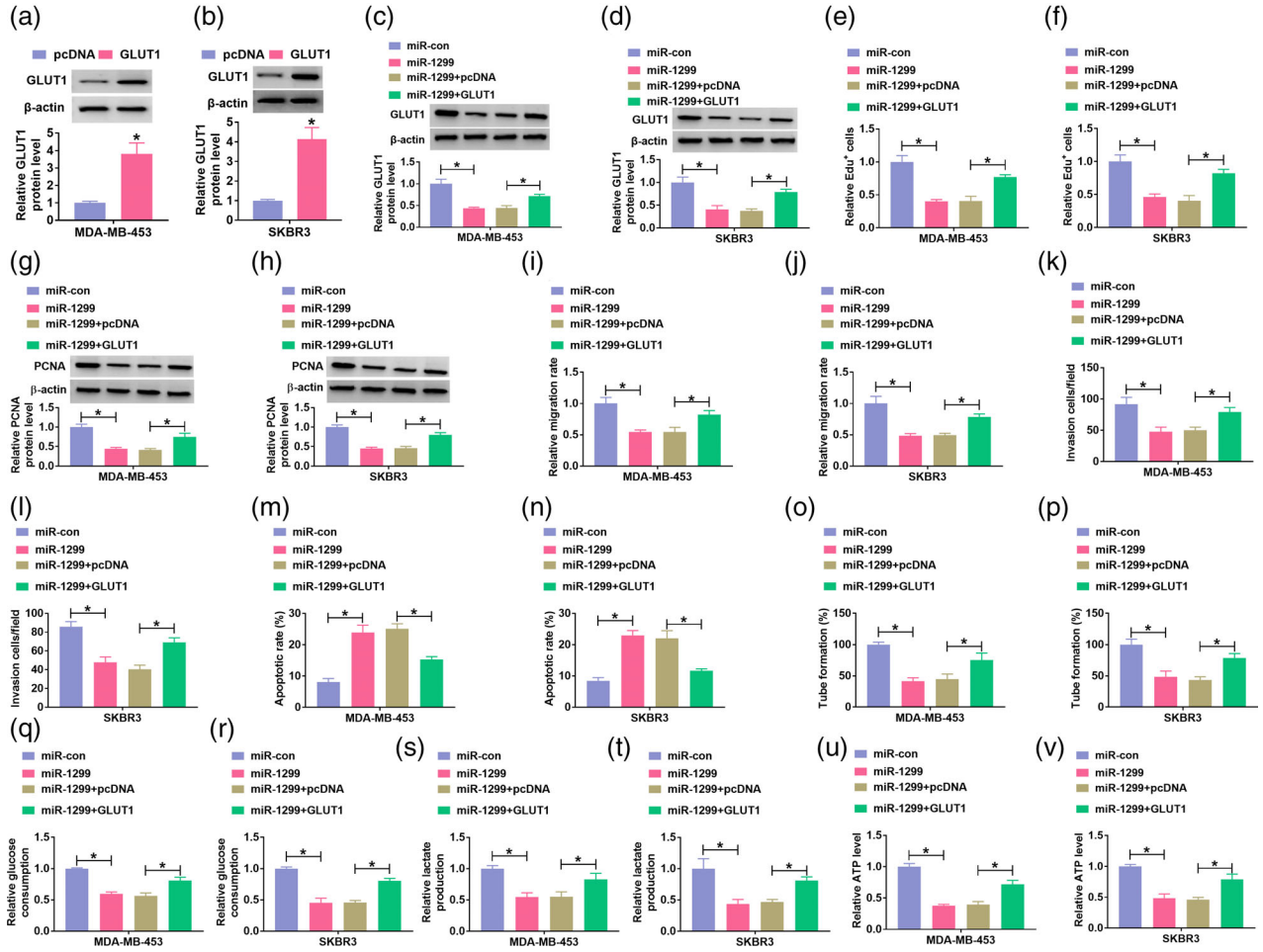

FIGURE 6 GLUT1 overexpression reversed the role of miR-1299 mimic. (a, b) The efficiency of GLUT1 overexpression was checked by western blot assay. (c, d) In MDA-MB-453 and SKBR3 cells transfected with miR-1299 or miR-1299 + GLUT1, GLUT1 protein level was measured by western blot. (e, f) Cell proliferation in these cells was assessed by EdU assay. (g, h) PCNA expression detected by western blot was used to assess cell proliferation. (i–l) Cell migration and cell invasion in these cells were evaluated by wound healing assay and transwell assay. (m, n) Cell apoptosis in these cells was evaluated by flow cytometry assay. (o–p) Angiogenesis in these cells was assessed by tube formation assay. (q–v) Glycolysis metabolism in these cells was evaluated by glucose consumption, lactate production and ATP level. *$p < 0.05$

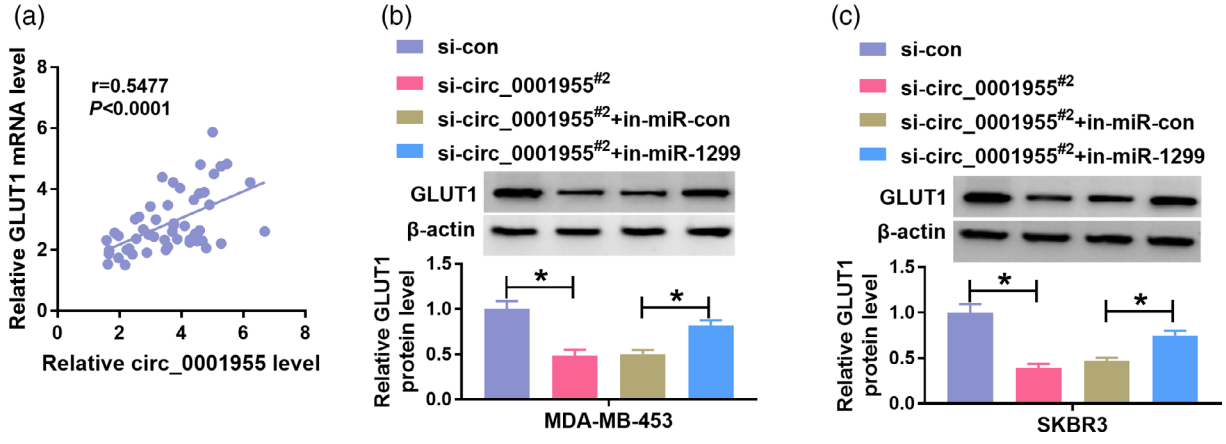

FIGURE 7 Circ_0001955 positively regulated GLUT1 expression via targeting miR-1299. (a) the correlation between GLUT1 expression and circ_0001955 expression in cancer tissues. (b, c) GLUT1 protein level in MDA-MB-453 and SKBR3 cells transfected with si-circ_0001955$^{\#2}$ or si-circ_0001955$^{\#2}$ + in-miR-1299 was measured by western blot. *$p < 0.05$

GLUT1 overexpression partly abolished the effect of miR-1299 (Figure 6o, p; Figure S2). Additionally, miR-1299 upregulation-depleted glucose consumption, lactate production and ATP content were all largely restored by GLUT1 overexpression (Figure 6q–v). The data advocated that miR-1299 inhibited breast cancer cell malignant properties via repressing GLUT1.

Circ_0001955 positively regulated GLUT1 expression via targeting miR-1299

Moreover, we discovered that GLUT1 mRNA expression in cancer tissues was positively correlated with circ_0001955 expression ($r = 0.5477$, $p < 0.0001$, Figure 7a). In addition, the expression of GLUT1 was notably declined in MDA-MB-453 and SKBR3 cells transfected with si-circ_0001955$^{\#2}$, while its expression was largely recovered in cells transfected with si-circ_0001955$^{\#2}$ + in-miR-1299 (Figure 7b, c). We concluded that circ_0001955 positively regulated GLUT1 expression via targeting miR-1299.

Circ_0001955 downregulation inhibited tumorigenesis in vivo

To verify the functional role of circ_0001955 in vivo, animal models were established in nude mice. The data in Figure 8a–c noticeably revealed that circ_0001955 downregulation slowed tumor growth, leading to poor tumor volume and weight. The expression of circ_0001955, miR-1299 and GLUT1 was then examined in the tumor tissues removed from the mice. The expression of circ_0001955 and GLUT1 protein was decreased, while the expression of miR-1299 was strengthened in tumor tissues removed from sh-circ_0001955-administered mice (Figure 8d–f). The data verified that circ_0001955 knockdown inhibited tumor growth via upregulating miR-1299 and downregulating GLUT1.

DISCUSSION

The considerable role of circRNA in cancer biology has previously been widely confirmed, and several circRNAs have been proposed as novel biomarkers and therapeutic targets for various cancers.[16] Our study investigated the role of circ_0001955 and discovered that circ_0001955 regulated breast cancer development via affecting cancer cell proliferation, migration, invasion, survival, angiogenesis and glycolysis metabolism. We further verified that circ_0001955 regulated breast cancer biology via positively modulating GLUT1 expression via acting as miR-1299 sponge. The data enriched the regulatory networks of circ_0001955 in breast cancer.

The carcinogenic role of circ_0001955 has been acknowledged in diverse cancers. RNA sequencing data identified that circ_0001955 was highly expressed in hepatocellular carcinoma (HCC) samples, which was verified by qPCR assay. In function, circ_0001955 overexpression promoted HCC cell proliferation and tumorigenesis in vivo.[17] Likewise, knockdown of circ_0001955 remarkably restrained HCC cell proliferation, migration, invasion and angiogenesis.[18,19] The upregulation of circ_0001955 has also been identified in colorectal cancer.[18] Interestingly, a GEO dataset (GSE101123) also illustrated that circ_0001955 was

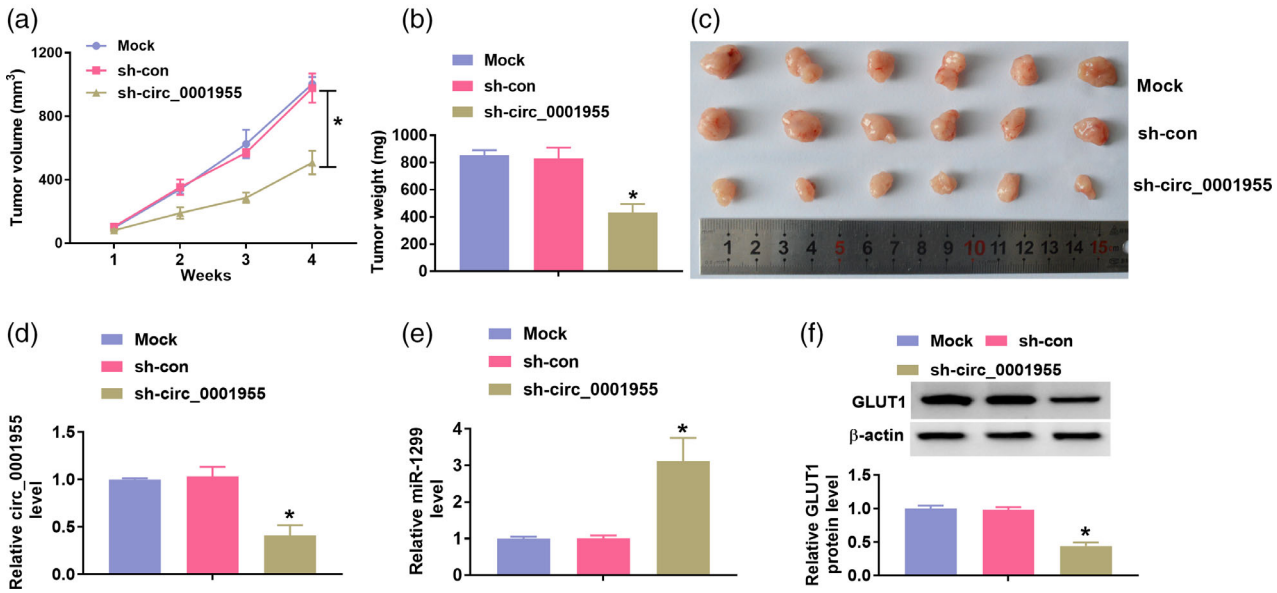

FIGURE 8 Circ_0001955 downregulation blocked tumor growth in vivo. (a–c) In animal models, tumor volume, tumor weight and tumor size were recorded to assess tumor growth. (d–f) The expression of circ_0001955, miR-1299 and GLUT1 in the removed tumor tissues was measured by qPCR or western blot. *$p < 0.05$

overexpressed in breast tumor tissues by RNA sequencing analysis, which was validated by qPCR data in our study. Consistent with previous studies,[18,19] we ensured that circ_0001955-silenced breast cancer cells had inhibitory cell proliferative, migratory and invasive capacities. The growth of solid tumors depends on blood vessels that provide nutrition and oxygen to the tumor.[20] In addition, aerobic glycolysis is a vital metabolic feature of tumor cells, which contributes to energy production and biosynthetic capability in tumor biology.[21] We thus assessed the role of circ_0001955 on angiogenesis and glycolysis metabolism, and silencing circ_0001955 largely suppressed the ability of angiogenesis and glycolysis in tumor cells. Moreover, the carcinogenic role of circ_0001955 was verified by animal study. These characteristics of circ_0001955 in breast cancer hinted that the targeted inhibition of circ_0001955 might be promising to prevent breast cancer development.

In previous studies, several miRNAs targeted by circ_0001955 have been identified.[17,18] Herein, miR-1299 was newly identified target of circ_0001955. We observed that miR-1299 harbored poor expression in breast tumor tissues and cells, which was consistent with previous findings.[22] In addition, miR-1299 was also determined to be targeted by several oncogenic circRNAs, such as circ_0136666 and circ_0006528, and these circRNAs promoted breast cancer cell growth, metastasis and chemoresistance via sequestering miR-1299 expression.[22,23] Additionally, poor expression of miR-1299 has also been observed in other cancers, such as HCC and ovarian cancer, and miR-1299 has been found to serve as a tumor suppressor to block the malignant development of these cancers.[24,25]

In our study, we identified that miR-1299 enrichment inhibited breast cancer cell proliferation, angiogenesis, migration, invasion and glycolysis. However, circ_0001955 acted as an miR-1299 sponge to sequester miR-1299 expression and attenuate the antitumor effect of miR-1299. The interaction between circ_0001955 and miR-1299 in breast cancer is for the first time proposed in our study.

GLUT1, encoded by SLC2A1, is a principal transporter of glucose and contributes to glycolysis metabolism in cancer development.[26] The aberrant upregulation of GLUT1 has frequently been observed in various cancers, including breast cancer.[27–29] In triple-negative breast cancer, GLUT1 targeted epidermal growth factor receptor and integrin signaling to accelerate cancer cell growth, migration and invasion.[30] In addition, GLUT1 facilitated glycolysis in breast cancer to aggravate cancer cell oncogenic phenotypes.[31] Knockdown of GLUT1 has also been shown to strengthen chemoresistance in breast cancer cells.[32] Consistent with previous data, we found that GLUT1 was overexpressed in breast cancer tissues and cells. In addition, the antitumor effects of miR-1299 enrichment, including proliferation, angiogenesis, migration, invasion and glycolysis, were all abolished by GLUT1 overexpression, thus verifiying the carcinogenic role of GLUT1.

In conclusion, in our study we determined that circ_0001955 is highly expressed in breast cancer. Deficiency of circ_0001955 blocked breast cancer development via depleting cancer cell proliferation, angiogenesis, migration, invasion and glycolysis, which was achieved by the regulation of miR-1299/GLUT1 pathway by circ_0001955. Our study addressed a new mechanism regarding circ_0001955 function in breast cancer, supporting the finding that targeted inhibition of circ_0001955 might be a therapeutic strategy for breast cancer.

CONFLICT OF INTEREST

The authors declare that they have no conflicts of interest.

ORCID

Shengrong Sun https://orcid.org/0000-0001-5581-9572

REFERENCES

1. Sung H, Ferlay J, Siegel RL, Laversanne M, Soerjomataram I, Jemal A, et al. Global cancer statistics 2020: GLOBOCAN estimates of incidence and mortality worldwide for 36 cancers in 185 countries. CA Cancer J Clin. 2021;71:209–49.
2. Al-Mahmood S, Sapiezynski J, Garbuzenko OB, Minko T. Metastatic and triple-negative breast cancer: challenges and treatment options. Drug Deliv Transl Res. 2018;8:1483–507.
3. Lobry C, Oh P, Mansour MR, Look AT, Aifantis I. Notch signaling: switching an oncogene to a tumor suppressor. Blood. 2014;123:2451–9.
4. Oliveira AM, Ross JS, Fletcher JA. Tumor suppressor genes in breast cancer: the gatekeepers and the caretakers. Am J Clin Pathol. 2005;124(Suppl):S16–28.
5. Mayer IA, Arteaga CL. The PI3K/AKT pathway as a target for cancer treatment. Annu Rev Med. 2016;67:11–28.
6. Tomar D, Yadav AS, Kumar D, Bhadauriya G, Kundu GC. Non-coding RNAs as potential therapeutic targets in breast cancer. Biochim Biophys Acta Gene Regul Mech. 2020;1863:194378.
7. Tang Q, Hann SS. Biological roles and mechanisms of circular RNA in human cancers. Onco Targets Ther. 2020;13:2067–92.
8. Li J, Sun D, Pu W, Wang J, Peng Y. Circular RNAs in cancer: biogenesis, function, and clinical significance. Trends Cancer. 2020;6:319–36.
9. Tang H, Huang X, Wang J, Yang L, Kong Y, Gao G, et al. circKIF4A acts as a prognostic factor and mediator to regulate the progression of triple-negative breast cancer. Mol Cancer. 2019;18:23.
10. Sang Y, Chen B, Song X, Li Y, Liang Y, Han D, et al. circRNA_0025202 regulates Tamoxifen sensitivity and tumor progression via regulating the miR-182-5p/FOXO3a Axis in breast cancer. Mol Ther. 2019;27:1638–52.
11. Su M, Xiao Y, Ma J, Tang Y, Tian B, Zhang Y, et al. Circular RNAs in cancer: emerging functions in hallmarks, stemness, resistance and roles as potential biomarkers. Mol Cancer. 2019;18:90.
12. Shang Q, Yang Z, Jia R, Ge S. The novel roles of circRNAs in human cancer. Mol Cancer. 2019;18:6.
13. Wu W, Ji P, Zhao F. CircAtlas: an integrated resource of one million highly accurate circular RNAs from 1070 vertebrate transcriptomes. Genome Biol. 2020;21:101.
14. Dudekula DB, Panda AC, Grammatikakis I, De S, Abdelmohsen K, Gorospe M. CircInteractome: a web tool for exploring circular RNAs and their interacting proteins and microRNAs. RNA Biol. 2016;13:34–42.
15. Gao A, Sun T, Ma G, Cao J, Hu Q, Chen L, et al. LEM4 confers tamoxifen resistance to breast cancer cells by activating cyclin D-CDK4/6-Rb and ERalpha pathway. Nat Commun. 2018;9:4180.
16. Lei B, Tian Z, Fan W, Ni B. Circular RNA: a novel biomarker and therapeutic target for human cancers. Int J Med Sci. 2019;16:292–301.
17. Yao Z, Xu R, Yuan L, Xu M, Zhuang H, Li Y, et al. Circ_0001955 facilitates hepatocellular carcinoma (HCC) tumorigenesis by sponging

miR-516a-5p to release TRAF6 and MAPK11. Cell Death Dis. 2019; 10:945.
18. Ding B, Fan W, Lou W. hsa_circ_0001955 enhances in vitro proliferation, migration, and invasion of HCC cells through miR-l145-5p/NRAS Axis. Mol Ther Nucleic Acids. 2020;22: 445–55.
19. Li X, Lv J, Hou L, Guo X. Circ_0001955 acts as a miR-646 sponge to promote the proliferation, metastasis and angiogenesis of hepatocellular carcinoma. Dig Dis Sci. 2021. https://doi.org/10.1007/s10620-021-07053-8
20. Wang Z, Dabrosin C, Yin X, Fuster MM, Arreola A, Rathmell WK, et al. Broad targeting of angiogenesis for cancer prevention and therapy. Semin Cancer Biol. 2015;35(Suppl):S224–S43.
21. Tang J, Luo Y, Wu G. A glycolysis-related gene expression signature in predicting recurrence of breast cancer. Aging (Albany NY). 2020; 12:24983–94.
22. Liu G, Zhang Z, Song Q, Guo Y, Bao P, Shui H. Circ_0006528 contributes to paclitaxel resistance of breast cancer cells by regulating miR-1299/CDK8 Axis. Onco Targets Ther. 2020;13: 9497–511.
23. Liu LH, Tian QQ, Liu J, Zhou Y, Yong H. Upregulation of hsa_circ_0136666 contributes to breast cancer progression by sponging miR-1299 and targeting CDK6. J Cell Biochem. 2019;120: 12684–93.
24. Zhu H, Wang G, Zhou X, Song X, Gao H, Ma C, et al. miR-1299 suppresses cell proliferation of hepatocellular carcinoma (HCC) by targeting CDK6. Biomed Pharmacother. 2016;83:792–7.
25. Pei Y, Li K, Lou X, Wu Y, Dong X, Wang W, et al. miR1299/NOTCH3/TUG1 feedback loop contributes to the malignant proliferation of ovarian cancer. Oncol Rep. 2020;44:438–48.
26. Zambrano A, Molt M, Uribe E, Salas M. Glut 1 in cancer cells and the inhibitory action of resveratrol as a potential therapeutic strategy. Int J Mol Sci. 2019;20:3374.
27. Ancey PB, Contat C, Boivin G, Sabatino S, Pascual J, Zangger N, et al. GLUT1 expression in tumor-associated neutrophils promotes lung cancer growth and resistance to radiotherapy. Cancer Res. 2021;81: 2345–57.
28. Meziou S, Ringuette Goulet C, Hovington H, Lefebvre V, Lavallée É, Bergeron M, et al. GLUT1 expression in high-risk prostate cancer: correlation with (18)F-FDG-PET/CT and clinical outcome. Prostate Cancer Prostatic Dis. 2020;23:441–8.
29. Wu Q, Ba-Alawi W, Deblois G, Cruickshank J, Duan S, Lima-Fernandes E, et al. GLUT1 inhibition blocks growth of RB1-positive triple negative breast cancer. Nat Commun. 2020;11:4205.
30. Oh S, Kim H, Nam K, Shin I. Glut1 promotes cell proliferation, migration and invasion by regulating epidermal growth factor receptor and integrin signaling in triple-negative breast cancer cells. BMB Rep. 2017;50:132–7.
31. Lin C, Xu X. YAP1-TEAD1-Glut1 axis dictates the oncogenic phenotypes of breast cancer cells by modulating glycolysis. Biomed Pharmacother. 2017;95:789–94.
32. Oh S, Kim H, Nam K, Shin I. Silencing of Glut1 induces chemoresistance via modulation of Akt/GSK-3beta/beta-catenin/survivin signaling pathway in breast cancer cells. Arch Biochem Biophys. 2017;636: 110–22.

SUPPORTING INFORMATION

Additional supporting information may be found in the online version of the article at the publisher's website.

How to cite this article: Cheng H, Kuang S, Tan L, Sun S. Circ_0001955 plays a carcinogenic role in breast cancer via positively regulating GLUT1 via decoying miR-1299. Thorac Cancer. 2022;13:913–24. https://doi.org/10.1111/1759-7714.14310